Journal of Solid State Chemistry **162,** 333–340 (2001)
doi:10.1006/jssc.2001.9331, available online at http://www.idealibrary.com on IDEAL®

Preparation, Magnetic Properties, and Pressure-Induced Transitions of Some $M^{II}M^{IV}F_6$ (M^{II} = Ni, Pd, Cu; M^{IV} = Pd, Pt, Sn) Complex Fluorides

Alain Tressaud*,[1] and Neil Bartlett†

*Institut de Chimie de la Matière Condensée de Bordeaux, ICMCB-CNRS, 87 Avenue du Dr A. Schweitzer, 33608 Pessac, France; and †Department of Chemistry, and Chemical Sciences Division, Lawrence Berkeley National Laboratory, University of California—Berkeley, Berkeley, California 94720
E-mail: tressaud@icmcb.u-bordeaux.fr

Received February 26, 2001; in revised form July 17, 2001; accepted August 1, 2001

IN HONOR OF PROFESSOR PAUL HAGENMULLER ON THE OCCASION OF HIS 80TH BIRTHDAY

$M^{II}M^{IV}F_6$ (M^{II} = Ni, Pd, Cu; M^{IV} = Pd, Pt) and $PdSnF_6$ complex fluorides have been synthesized via different preparative methods using either BrF_3 as oxidizer and solvent, or solid state reactions. For M^{II} = Ni, Pd, the phases crystallize in the rhombohedral space group $R\bar{3}$ ($LiSbF_6$ type). Cationic ordering has been studied by X-ray diffraction and ^{119}Sn Mössbauer resonance for $PdSnF_6$. A lowering of symmetry has been observed when the involved divalent cation presents a Jahn–Teller configuration (Cu^{II}). Except for $PdSnF_6$, which is paramagnetic down to 4 K, all compounds are Pd_2F_6-type ferromagnets at low temperature. This behavior has been related to the ordering between half-filled e_g orbitals of the divalent cation and empty e_g orbitals of the tetravalent cation. A drastic increase in conductivity has been observed under high pressures. In particular the insulator–semiconductor transition induced under pressure (up to 80 kbar) in Pd_2F_6 corresponds to a decrease of the electrical resistivity by six orders of magnitude. The assumption of an electronic transition induced under pressure from mixed oxidation states ($M^{II} + M^{IV}$) to an unique trivalent M^{III} oxidation state has been proposed.

Key Words: ***$M^{II}M^{IV}F_6$; transition element fluorides; BrF_3 medium; solid state reaction; ferromagnetism; pressure-induced electronic transition; piezosensors.***

INTRODUCTION

In recent years, investigations have been carried out on $M^{II}M^{IV}F_6$ compounds (M^{II} and/or M^{IV} are transition elements), the networks of which generally derive from that of ReO_3. The arrangement corresponds to a NaCl-type packing of ($M^{II}F_{6/2}$) and ($M^{IV}F_{6/2}$) octahedra. Several structural types have been proposed, depending on the presence (or not) of a cationic ordering (see, for instance, (1, 2)).

The rhombohedral $LiSbF_6$-type (space group $R\bar{3}$), with an ordering of the metal ions, is most commonly found at room temperature. In many of these $M^{II}M^{IV}F_6$ compounds a structural phase transition to a high-temperature form of the $NaSbF_6$ type, which exhibits cubic symmetry (space group $Fm\bar{3}m$), occurs. For a random cationic distribution, the rhombohedral VF_3 type (space group $R\bar{3}c$), in which the fluorine–ligand stacking is intermediate between fcc packing with vacancies and hc packing, is found. With respect to the ReO_3 prototype, ($MF_{6/2}$) octahedra in the VF_3 type are slightly rotated around their threefold axis and F ligands are therefore shifted from the edges of the pseudo-cell.

When the M sites are occupied by the same metal the choice between the space groups $R\bar{3}$ ($LiSbF_6$ type, with two different ordered oxidation states) and $R\bar{3}c$ (VF_3 type with two different disordered oxidation states or two M^{III}) is not readily predictable, and the unit cells are nearly the same. An instance of the difficulty was the clarification by Bartlett and Rao (3) that the fluoride longly described as "palladium trifluoride" was the mixed oxidation state compound $Pd^{II}Pd^{IV}F_6$. This resolved the conflict between an essentially octahedral fluorine–ligand environment of palladium atoms as described by Jack and co-workers (4) and the value of the magnetic moment, interpreted by Nyholm and Sharpe (5) as indicative of a low-spin d^7 configuration for the supposed Pd^{III}. When there is an unequal occupancy of the antibonding e_g orbitals of the M transition element, a lowering in symmetry due to the Jahn–Teller effect is expected to occur, although metastable rhombohedral materials (e.g., $Ag^{II}Pd^{IV}F_6$, $Ag^{II}Pt^{IV}F_6$) may be preparable by low-temperature methods (6).

This work deals with the preparative methods and the structural, magnetic, and pressure-induced features of some $M^{II}M^{IV}F_6$ complex fluorides with M^{II} = Ni, Pd, Cu and M^{IV} = Pd, Pt, Sn.

[1]To whom correspondence should be addressed. Fax: (33)5 56 84 27 61.

0022-4596/01 $35.00

EXPERIMENTAL

Preparative Methods

The preparative methods used in this study have been described previously for both the bromine trifluoride oxidizer and solvent (7), and for the solid state approach (8). The description of the metal fluoride handling and disposal lines can also be found in previous articles (9). Since the final compounds are sensitive to moisture, their preparation and their handling requires strict exclusion of moisture.

Materials

$PdBr_2$. This compound was prepared by dissolution of spectroscopically certified high-purity palladium sponge (Johnson, Matthey, and Mallory, Ltd, Toronto, Canada) in AR grade 48% hydrobromic acid to which freshly distilled bromine was added as oxidant. Following evaporation to dryness, the dark brown residue was dried at 70°C in a dynamic vacuum. (Found = Pd 39.5, $PdBr_2$ required 39.9%.) *Bromine trifluoride* from the Matheson Co., East Rutherford, NJ, was subjected to trap distillation, the more volatile fractions were discarded, and only clear yellow liquid was employed in the synthetic work. *Platinum tetrabromide* was prepared by Halberstadt's modification of the method of Meyer and Zublin (Found: Pt, 38.3; $PtBr_4$ requires: Pt, 37.9%).

$Pd^{II}Pd^{IV}F_6$. This compound was prepared in two ways. Interaction of $PdBr_2$ with BrF_3 yielded the bromine trifluoride adduct $PdF_3 \cdot BrF_3$ (10), from which Pd_2F_6 was obtained as described by Sharpe (11) by decomposing at 220°C in a quartz container, under vacuum. The black solid (Found: F, 34.2; Pd, 65.1; Calc. for Pd_2F_6: F, 34.8; Pd, 65.2%), was characterized by X-ray powder diffraction, all lines being characteristic of the pattern described by Jack and coworkers (4). Other samples of Pd_2F_6 were prepared by direct fluorination of palladium sponge (12). Several 8-h fluorinations (pressure 1 atm.) at 500°C were necessary to obtain Pd_2F_6 free of PdF_2 (by X-ray diffraction). Between the fluorination cycles, the material was ground in a glove box containing less than 2 ppm H_2O and O_2.

$Pd^{II}Pt^{IV}F_6$. This compound was also prepared both from BrF_3 solution and solid state reaction. Dissolution of equimolar quantities of $PdBr_2$ and $PtBr_4$ in BrF_3 yielded a red-brown solution. Removal of volatiles in a dynamic vacuum left a brown solid that became light brown when heated *in vacuo* to 180°C. This product was rendered more crystalline by heating it in fluorine (1 atm.) to 200°C in a monel vessel. Analysis was by pyrohydrolysis. The total palladium and platinum content was obtained by reduction in hydrogen to 400°C, and the palladium was separately determined as the dimethyl glyoxime complex (Found: F, 27.0; Pd, 25.1; Pd + Pt, 72.9; $PdPtF_6$ requires: F, 27.4; Pd, 25.6 Pd + Pt, 72.6%). X-ray powder data were indexed on the basis of a primitive rhombohedral unit cell $a = 5.55(1)$ Å, $\alpha = 54.00(2)^\circ$, $V = 103.8$ Å^3, $Z = 1$. Solid state synthesis from stoichiometric mixtures of PdF_2 and PtF_4 were carried out in sealed platinum tubes at 500°C. PdF_2 was prepared after the method of Müller and Hoppe (13), and PtF_4 was obtained according to the reaction $4PtF_5 + Pt \rightarrow PtF_4$ in sealed platinum tubes at 400°C under N_2. This method yielded $PdPtF_6$ crystallographically identical to that obtained from BrF_3 solution (3, 14).

$Pd^{II}Sn^{IV}F_6$. The interaction of BrF_3 with equimolar mixtures of $PdBr_2$ and either SnI_4 (very vigorous!) or $SnBr_4$ yielded a red-brown solution. Volatiles were removed in a dynamic vacuum and the resulting brown solid was heated *in vacuo* to 180°C. Analysis was by pyrohydrolysis at 300°C. Tin was determined as the oxide. (Found: F, 32.6; Sn, 35.5; Pd, 31.9. $PdSnF_6$ requires: F, 33.6; Sn, 35.0; Pd, 31.4%.) A solid state synthesis from PdF_2 and SnF_4 carried out as described for $PdPtF_6$ yielded material crystallographically indistinguishable from that obtained from BrF_3 solution. X-ray powder data were indexed on the basis of a primitive rhombohedral unit cell (space group $R\bar{3}$) with $a = 5.70(2)$ Å; $\alpha = 53.13(5)^\circ$; $V = 110.0$ Å^3, $Z = 1$ (14).

$M^{II}Pd^{IV}F_6$ and $M^{II}Pt^{IV}F_6$ with M^{II} = Ni and Cu. These compounds were synthesized in sealed platinum tubes by solid state reaction between NiF_2 or CuF_2 and PdF_4 or PtF_4. The reactions were carried out in the temperature range 400–600°C, depending on the compound to be prepared. The final materials were characterized by X-ray diffraction.

Characterizations

X-ray diffraction. The symmetry and unit-cell constants of the different $M^{II}M^{IV}F_6$ compounds were determined using X-ray diffractometry. Because of their high reactivity, the samples were studied using either the Debye–Scherrer method with sealed quartz capillaries or alternatively the Bragg–Brentano method using an air-tight cell with Teflon O-rings and a Mylar window, both containers being filled in a dry box.

Magnetism. The magnetic properties have been determined on powdered samples from 4.2 to 300 K. A vibrating sample magnetometer, Faraday microbalance, and SQUID device have been used. To obtain precise values of the ordering temperatures and saturation magnetizations of the ferromagnetic materials, measurements were also made at Service National des Champs Intenses (CNRS-Grenoble, France). An extraction method was used down to 1.6 K under applied magnetic fields up to 15 T.

Electrical conductivity. For conductivity measurements at ambient pressure, the compound was compressed to

a cylindrical pellet. Two Cu electrodes with welded electrical wires were set on both sides. This pellet was placed in a Teflon matrix and covered with powdered Teflon (15). The arrangement was pressed up to 500 bar and sintered in order to ensure a waterproof cell. With such an encapsulated sample, electrical measurements were satisfactorily performed up to 550 K.

Piezoresistive properties of $M^{II}M^{IV}F_6$ compounds were studied using a belt-type unit, able to reach 90 kbar. The pressure dependence of the resistivity was followed *in situ* using a cell specially designed for the purpose (16). The cell was composed of a cylindrical pyrophyllite body with two Teflon O-rings. The sample was compressed in a dry box to form a pellet of 2.5 mm diameter. In order to prevent hydrolysis, it was coated with AlF_3. This unit was inserted in a Pt microfurnace. Between the furnace and the pyrophyllite body was set an additional protective layer of La_2O_3 (16, 17).

^{119}Sn Mössbauer spectroscopy. The source was $Ca^{119}SnO_3$ of 5 mCi activity at room temperature. The speed scale was calibrated using the value 2.57 mm·s^{-1} for the $BaSnO_3$–β Sn separation (18–20). The superficial weight of the $PdSnF_6$ sample was 7 mg·cm^{-2}. This value corresponded to a full-width at half-maximum (FWHM) of less than 0.90 mm·s^{-1} for the resonance line of $BaSnO_3$.

STRUCTURAL FEATURES OF $M^{II}M^{IV}F_6$ COMPOUNDS

Most of the transition element trifluorides crystallize in the rhombohedral space group $R\bar{3}c$ (VF_3 type). The F-ligand arrangement can be described as a compact stacking perpendicular to the [111] direction of the rhombohedron. Depending on the size of the transition element, this stacking varies from a fcc packing with one absent F-ligand over four layers to an hc packing. RhF_3, IrF_3, and the so-called "PdF_3" correspond to the hc limit (F_4 position: $x = -0.083$). The PdF_3 type has been considered since the classification made by Jack (4) as one of the main structural types of the transition metal trifluorides. The compound was first prepared by Sharpe in 1950 (11). In 1964, Bartlett and Rao suggested that PdF_3 was in fact $Pd^{II}Pd^{IV}F_6$, due to the absence of a Jahn–Teller distortion that is generally associated with d^7 cations in a low-spin state that tend to octahedral coordination (3). Early X-ray and neutron diffraction studies did not detect two different crystallographic environments for Pd^{II} and Pd^{IV} respectively (4, 21). A neutron diffraction study on powdered Pd_2F_6 (12) confirmed that the compound was of the $LiSbF_6$ type (space group $R\bar{3}$), with an ordering between Pd^{II} and Pd^{IV} species. The fluorine atom positions (6f sites) are $x = -0.109$, $y = 0.569$, $z = 0.273$. The corresponding distances are Pd^{II}–F = 2.17 Å and Pd^{IV}–F = 1.90 Å, proving the existence of two different types of ($PdF_{6/2}$) octahedra.

TABLE 1
Unit-Cell Constants and Symmetry of $M^{II}M^{IV}F_6$ Compounds

	M^{II}		
M^{IV}	Ni^{II}	Pd^{II}	Cu^{II}
Pd^{IV}	Rhombohedral $R\bar{3}$ $a = 5.37(1)$ Å $\alpha = 54.65(2)^\circ$ $Z = 1$	Rhombohedral $R\bar{3}$ $a = 5.52(1)$ Å $\alpha = 53.90(2)^\circ$ $Z = 1$	Triclinic $P\bar{1}$ $a = 4.971(1)$ Å $b = 5.015(1)$ Å $c = 9.523(3)$ Å $\alpha = 89.73(1)^\circ$ $\beta = 104.16(1)^\circ$ $\gamma = 121.49(1)^\circ$ $Z = 2$
	(23)	(3, 12)	(24)
Pt^{IV}	Rhombohedral $R\bar{3}$ $a = 5.38(1)$ Å $\alpha = 54.61(2)^\circ$ $Z = 1$	Rhombohedral $R\bar{3}$ $a = 5.55(1)$ Å $\alpha = 54.00(2)^\circ$ $Z = 1$	Triclinic $P\bar{1}$ $a = 4.952(1)$ Å $b = 4.985(1)$ Å $c = 9.624(3)$ Å $\alpha = 89.98(2)^\circ$ $\beta = 104.23(2)^\circ$ $\gamma = 120.35(2)^\circ$ $Z = 2$
	(25)	(3, 14)	(22)

X-ray powder data have shown $NiPdF_6$, $NiPtF_6$, $PdPtF_6$, and $PdSnF_6$ to be isostructural with Pd_2F_6. A lowering of the symmetry down to the $P\bar{1}$ triclinic space group is observed in the case of Jahn–Teller divalent cations such as Cu^{II} and Ag^{II}, at least when the compounds are obtained via solid state reactions. The structure type is that of $CuPtF_6$, and the unit-cell constants are derived from the hexagonal-cell alternative for the rhombohedral cell (22). Crystallographic data of $M^{II}Pd^{IV}F_6$ and $M^{II}Pt^{IV}F_6$ compounds with M^{II} = Ni, Pd, Cu are collected in Table 1. It can be added that, when they are prepared at the higher temperatures used for the preparation of $CuPtF_6$. $AgPdF_6$ and $AgPtF_6$ also crystallize in the triclinic space group $P\bar{1}$, and appear to be isostructural with the Cu^{II} compound.[2]

MÖSSBAUER RESONANCE STUDY OF $PdSnF_6$

Mössbauer spectra at 4.2 and 78 K of $PdSnF_6$ prepared by solid state synthesis are shown in Fig. 1. At room temperature, no resonance can be observed, even after counting times longer than 24 h. This phenomenon is certainly due to the important dependence of the recoilless absorption factor of ^{119}Sn in $PdSnF_6$. Mössbauer data have been fitted using a least-squares program (26) (Table 2). The negative value

[2]Private communication from B. G. Müller, Justus-Liebig-Universität, Giessen, Germany, 1998. Two important articles appeared recently on the crystal chemistry and potential superconductivity in Ag^{II} flourides: R. Fischer and B. G. Müller, *Z. Anorg. Allg. Chem.* **627,** 445 (2001) and W. Grochala and R. Hoffman, *Angew. Chem. Int. Ed.* **40,** 2742 (2001).

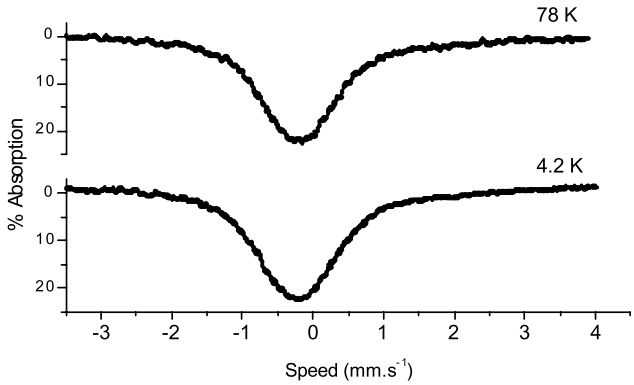

FIG. 1. Mössbauer spectra of $PdSnF_6$ at 78 and 4.2 K.

($\delta = -0.28\ \text{mm}\cdot\text{s}^{-1}$) of the isomer shift of $PdSnF_6$ relative to $BaSnO_3$ characterizes tetravalent tin in a fluoride ion environment (18, 19). The presence of Sn^{2+} species, whose isomer shift would be about $+3.2\ \text{mm}\cdot\text{s}^{-1}$ (19), was not detected. These results unequivocally confirm the formula $Pd^{II}Sn^{IV}F_6$.

Although no quadrupole splitting clearly appears in Fig. 1, the fitting of the spectra on the basis of one Lorentzian peak leads to important FWHM. These values, and also the statistical error, can be notably reduced, if the calculations are carried out on the basis of a Lorentzian doublet instead of a singlet. The values of the quadrupole splitting obtained from this second hypothesis are also given in Table 2. This splitting would arise from the presence of the cationic ordering. The absence of hyperfine magnetic interactions down to 4.2 K has been confirmed by the magnetic results.

MAGNETIC PROPERTIES OF $M^{II}M^{IV}F_6$ COMPOUNDS

Ferromagnetism in Pd_2F_6 and Related Compounds

The temperature dependence of the magnetization and the reciprocal susceptibility of Pd_2F_6 and $PdPtF_6$ are shown

TABLE 2
Mössbauer Data of $PdSnF_6$

	T(K)	δ ($\text{mm}\cdot\text{s}^{-1}$)	Δ ($\text{mm}\cdot\text{s}^{-1}$)	Γ ($\text{mm}\cdot\text{s}^{-1}$)
Lorentzian singlet	78	-0.28 ± 0.01	—	1.20 ± 0.02
	4.2	-0.28 ± 0.01	—	1.28 ± 0.02
Lorentzian doublet (with quadrupole splitting)	78	-0.28 ± 0.01	0.42 ± 0.01	0.98 ± 0.02
	4.2	-0.28 ± 0.01	0.45 ± 0.01	1.05 ± 0.02

Note. δ = isomer shift relative to $BaSnO_3$ at room temperature. Δ = quadrupole splitting. Γ = FWHM.

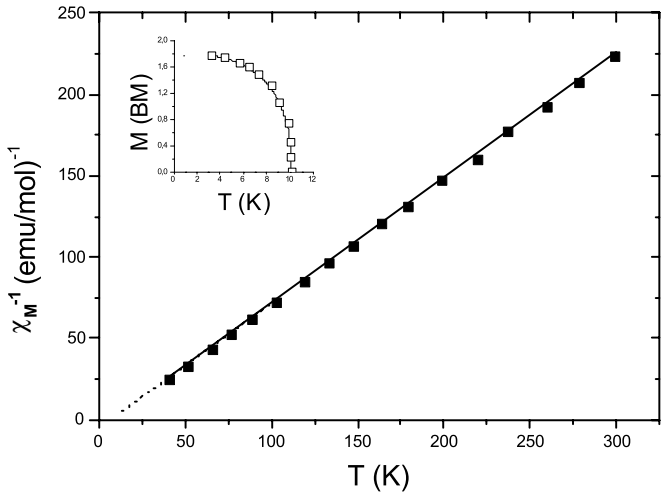

FIG. 2. Temperature dependence of the magnetization and reciprocal susceptibility of Pd_2F_6.

in Fig. 2 and Fig. 3. These variations fully characterize a ferromagnetic behavior. The values of the saturation magnetization and of the Curie temperatures are obtained using the method of Belov-Gozyaga (27) and Kouvel (28) from $M = f(1/H)$ and $M^2 = f(H/M)$ curve.

In Table 3 are summarized the magnetic data of Pd_2F_6-type ferromagnets. In the paramagnetic state the effective moment is due to the contribution of the M^{II} cations alone, since the M^{IV} elements are diamagnetic. All these ferromagnetic materials are characterized by a three-dimensional ordering between tetravalent cations with empty e_g orbitals (Pd^{IV} and Pt^{IV} in the low-spin t_{2g}^6 configuration) and divalent cations with high-spin $t_{2g}^6 e_g^2$ configuration. Superexchange couplings involving e_g electrons of the

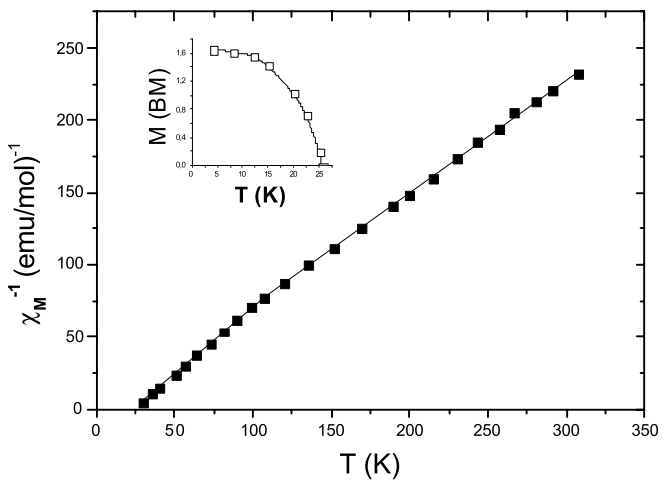

FIG. 3. Temperature dependence of the magnetization and reciprocal susceptibility of $PdPtF_6$.

TABLE 3
Magnetic Data of Pd_2F_6-Type Ferromagnets

Compound	T_C (K)	M_{sat} (BM) at 4.2 K	Θ_p (K)	C_{mol}
$NiPdF_6$	6.0(0.5)	1.42 (0.05)	4	1.32
$NiPtF_6$	8.0(0.5)	1.10 (0.10)	4	1.31
Pd_2F_6	10.0(0.5)	1.80 (0.10)	8	1.33
$PdPtF_6$[14]	25.0(0.5)	1.70 (0.10)	6	1.26
Pt_2F_6[29]	16.0(0.5)	1.60 (0.10)	18	1.20

divalent cations are responsible for the ferromagnetic behavior. One electron from a half-occupied e_g level of M^{II} is transferred without spin changing on an empty e_g level of Pd^{IV} and Pt^{IV} via p anionic orbitals. Both delocalization and correlation mechanisms are ferromagnetic.

Below the Curie temperature, the magnetic contribution to the neutron diffraction spectrum of Pd_2F_6 does not bring any new diffraction line but only an increase in some intensities: both nuclear and magnetic cells are identical (12). Due to a magnetic contribution to the [111] line, Pd^{II} moments cannot be parallel to the threefold symmetry axis. The best agreement between observed and calculated intensities is obtained when the direction of these moments is set perpendicular to this axis. A similar orientation has been previously observed for antiferromagnetic FeF_3 (30). The moment of divalent palladium, calculated using the form factor of Pd^{2+} free ion (31), is 1.75 BM. This in good agreement with the value found from the magnetic results.

When the involved divalent cation is Cu^{II}, the magnetic couplings are much lowered, because of the presence of an unique electron on the e_g orbitals and also of the resulting distortion of the octahedra. The field dependence of the magnetization at low temperatures (below 30 K) is shown in Fig. 4 for $CuPdF_6$ and $CuPtF_6$. It appears that a saturation phenomenon does not occur above 10 K, even under very high applied magnetic fields. It can be noted that similar behavior has been observed for $AgPdF_6$ and $AgPtF_6$. For $CuPdF_6$ the magnetization at 1.7 K under 15 T reaches the expected value ($M_{sat} = 1$ BM) for a $3d^9$ electronic configuration. On the other hand a much lower value, i.e., $M_{sat} \approx 0.40$ BM, is observed for $CuPtF_6$ under the same conditions.

The temperature dependences of the reciprocal susceptibilities of $CuPdF_6$ and $CuPtF_6$ are grouped in Fig. 5 and illustrate the absence of three-dimensional interactions down to 10 K. The T_C values have been estimated from $M^2 = f(H/M)$ curves, but a determination of the magnetic structure by neutron diffraction is required to get precisely the ordering temperatures.

$PdSnF_6$

Concerning $PdSnF_6$, since no d orbital is near the frontier-orbital levels in Sn^{IV}, the magnetic couplings between the paramagnetic elements are extremely weak. Paramagnetic behavior is therefore observed for $PdSnF_6$ down to 4.2 K (χ_M^{-1} (300 K) = 240.5 emu; $M_{eff} = 3.33\ \mu_B$; $\Theta_p = -34$ K; $C_{mol} = 1.39$). The absence of three-dimensional couplings furthermore confirms the results by Mössbauer spectroscopy. This behavior is like that of $PdGeF_6$ (32).

ELECTRONIC TRANSITIONS INDUCED UNDER PRESSURE

At ambient pressure, the insulating properties of $M^{II}M^{IV}F_6$ compounds have been confirmed by electrical measurements. Resistivity and activation energies are about 10^{10} Ω·cm and 1.5 eV respectively.

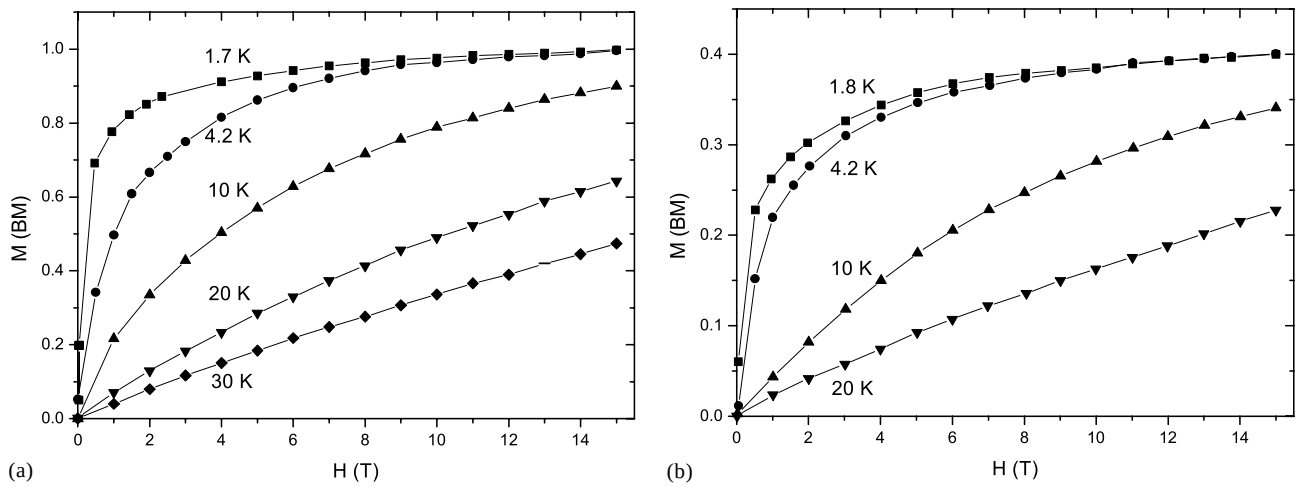

FIG. 4. Magnetic field dependence of the magnetization of (a) $CuPdF_6$ and (b) $CuPtF_6$.

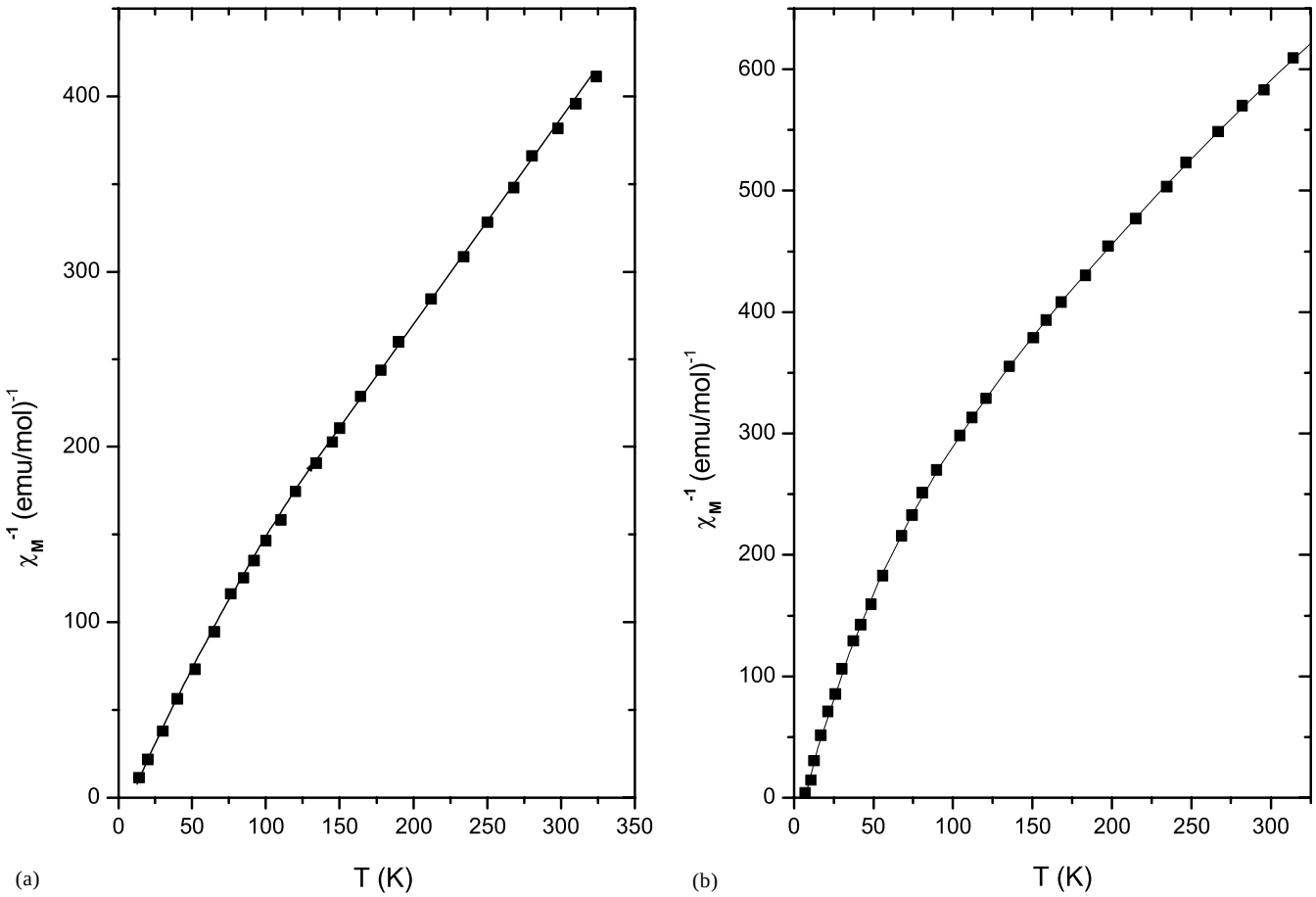

FIG. 5. Temperature dependence of the reciprocal susceptibility of (a) $CuPdF_6$ and (b) $CuPtF_6$.

The pressure dependence of the resistivity (ρ) of Pd_2F_6 at 25°C is represented in Fig. 6. Resistivity values decrease by six orders of magnitude up to 80 kbar. A linear dependence of $\log\rho$ with P is observed below 25 kbar: $d\log\rho/dP = -0.18\,\text{kbar}^{-1}$; from 50 to 85 kbar the slope is $d\log\rho/dP = -0.015\,\text{kbar}^{-1}$. The material could be proposed as a pressure sensor because of its linear response of resistivity variation in large pressure ranges. When pressure is unloaded, the initial resistivity is recovered after a hysteresis process. The evolution of the activation energy with pressure has been measured by heating and cooling cycles under a given pressure at various temperatures from room temperature to about 250°C. A hysteresis phenomenon is observed between ρ values measured during the heating cycle and those measured during the successive cooling cycle. This effect decreases with increasing pressure. The activation energy determined from the slope of the cooling cycle drastically diminishes with applied pressure: for $P = 20$ kbar, ΔE is equal to 0.24 eV and for $P = 60$ kbar, ΔE is as low as 0.07 eV (16). For both types of measurements, i.e., $d\log\rho = f(P)$ at T constant and $d\log\rho = f(T)$ at P constant, the materials have been surveyed by X-ray diffraction after every quenching cycle.

The drastic decrease in resistivity of Pd_2F_6 can be attributed to a movement of the fluoride ions toward the center of the Pd^{II}–Pd^{IV} bonds. Every palladium atom would tend to have identical environment with a lowering of the Franck–Condon barrier to intervalence electron transfer. This would correspond to the reaction $Pd^{II} + Pd^{IV} \Leftrightarrow 2Pd^{III}$. Similar hypotheses have been proposed to account for the important piezosensitive properties of $CsAuCl_3$, which is a $Au^{I} + Au^{III}$ compound under ambient conditions (33). Concerning the pressure dependence of the energy diagram, in addition to a decrease of the gap between Pd^{II} and Pd^{IV} e_g levels, new e_g^I Pd^{III} levels would appear. A hopping mechanism would arise between Pd^{II} and Pd^{III} species and also between Pd^{III} and Pd^{IV}. The values of the activation energies observed at high pressures are similar to those of semiconductor oxides showing hopping properties. However, the still important value of the resistivity ($10^4\,\Omega\cdot$cm) could be explained by a lower mobility of the localized electrons. It has proved to be impossible to obtain genuine $Pd^{III}F_3$ at

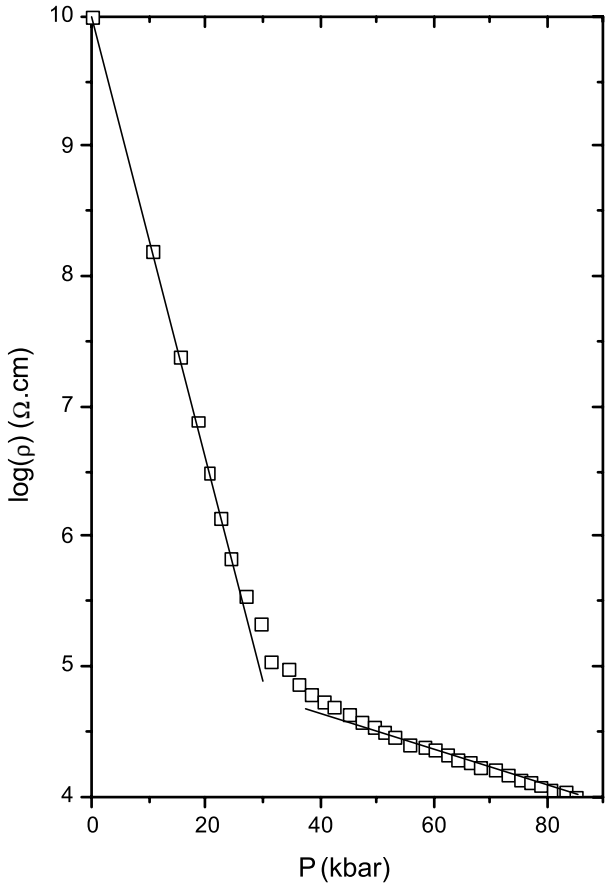

FIG. 6. Pressure dependence of the resistivity of Pd_2F_6 at 25°C.

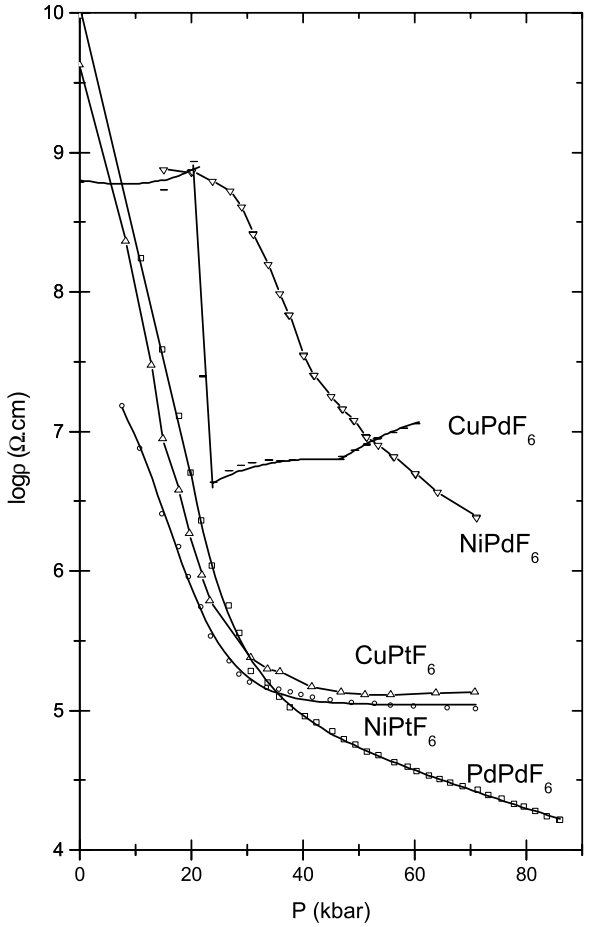

FIG. 7. Pressure dependence of resistivity for some $M^{II}M^{IV}F_6$ compounds at 25°C.

ambient pressure, even for quenched samples. However the hypothesis of the formation of Pd^{III} species under high pressures is supported by the existence of genuine Pd^{III} fluorocompounds with ordered perovskite (elpasolite) structure (34).

A drastic increase in conduction is observed when other $M^{II}M^{IV}F_6$ compounds are submitted to high pressure as shown in Fig. 7. The importance of the transition gap seems to be correlated to the extension of the participating metal orbitals. The difference between the resistivity under room pressure and that under 80 kbar is of five to six orders of magnitude when $4d$–$4d$ orbitals (Pd_2F_6), or $3d$–$5d$ orbitals ($NiPtF_6$, $CuPtF_6$) are involved, whereas a difference of about two orders of magnitude is observed in the $3d$–$4d$ case ($NiPdF_6$, $CuPdF_6$). Since all these phases contain M^{II} elements with half-filled e_g orbitals and M^{IV} elements with empty e_g orbitals, an electronic transition similar to that occurring in Pd_2F_6 can be assumed. It should be noted that the lowest activation energy is found when the same element is present in two oxidation states. At 70 kbar, ΔE is lower than 0.07 eV for Pd_2F_6, whereas it is about 0.18 eV for $NiPtF_6$ and $CuPtF_6$, and about 0.45 eV for $NiPdF_6$. Evidently the postulated orbital overlap is best when the d orbitals are of the same principal quantum number, poorer for $3d$–$4d$, and poorest for $3d$–$5d$.

ACKNOWLEDGMENTS

P. Hagenmuller, R. C. Sherwood, and G. Demazeau are acknowledged for fruitful discussions, F. Langlais for his contribution in the measurements of conductivities under high-pressure conditions, F. Ménil and L. Fournès for Mössbauer investigations, and L. Lozano for his competences in fluorination techniques. NATO is also acknowledged for a postdoctoral fellowship to A.T. in 1972 that allowed to start at that time the cooperation between Bordeaux and Berkeley on these topics. The work at Berkeley was supported by the Director, Office of Energy Research, by the Office of Basic Energy Sciences, and by the Chemical Sciences Division of the U.S. Department of Energy under Contract DE-AC03-67SF00098.

REFERENCES

1. D. Reinen and F. Steffens, *Z. Anorg. Allg. Chem.* **441,** 63 (1978).
2. D. Babel and A. Tressaud, *in* "Inorganic Solid Fluorides" (P. Hagenmuller, Ed.), Chap. 3, p. 77. Academic Press, New York, 1985, and references cited therein.
3. N. Bartlett and P. R. Rao, *Proc. Chem. Soc.* 383 (1964).

4. M. A. Hepworth, K. M. Jack, R. D. Peacock, and G. J. Westland, *Acta Crystallogr.* **10,** 63 (1957).
5. R. S. Nyholm and A. G. Sharpe, *J. Chem. Soc.* 3579 (1952).
6. O. Graudejus, S. H. Elder, G. M. Lucier, C. Shen, and N. Bartlett, *Inorg. Chem.* **38,** 2503 (1999).
7. N. Bartlett, *in* "Preparative Inorganic Reactions" (W. L. Jolly, Ed.), Vol. 3, p. 301. Interscience New York, 1965, and references cited therein.
8. R. Bougon, J. Erehtsman, J. Portier, and A. Tressaud, *in* "Preparative Methods in Inorganic Chemistry" (P. Hagenmuller, Ed.) Chap. 10, p. 401. Academic Press, New York, 1977.
9. J. Grannec and L. Lozano, *in* "Inorganic Solid Fluorides" (P. Hagenmuller, Ed.), Chap. 2, p. 18. Academic Press, New York, 1985, and references cited therein.
10. O. Ruff and E. Ascher, *Z. Anorg. Allg. Chem.* **183,** 193 (1929).
11. A. G. Sharpe, *J. Chem. Soc.* 3444 (1950).
12. A. Tressaud, M. Wintenberger, N. Bartlett, and P. Hagenmuller, *C. R. Acad. Sci.* **282,** 1069 (1976).
13. B. G. Müller and R. Hoppe, *Mater. Res. Bull.* **7,** 1297 (1972).
14. A. Tressaud, R. C. Sherwood, J. Portier, N. Bartlett, and P. Hagenmuller, *in* "Proceedings VIIIth International Symposium on Fluorine Chemistry, Kyoto, Japan, 1976."
15. A. Tressaud, F. Langlais, G. Demazeau, C. Lucat, J. M. Réau, J. Portier, and P. Hagenmuller, *Marché Innovation* (France) **43,** 20 (1980).
16. F. Langlais, G. Demazeau, J. Portier, A. Tressaud, and P. Hagenmuller, *Solid. State Commun.* **29,** 473 (1979).
17. G. Demazeau, Doctorate Thesis, Université Bordeaux, France, 1973.
18. F. W. D. Woodham, R. A. Howie, and O. Knop, *Can. J. Chem.* **52,** 1904 (1974).
19. N. N. Greenwood and T. C. Gibb, "Mössbauer Spectroscopy." Chapman and Hall, London, 1971.
20. D. E. Williams and C. W. Kocher, *J. Chem. Phys.* **52,** 1480 (1970).
21. M. K. Wilkinson, E. O. Wollan, H. R. Child, and J. W. Cable, *Phys. Rev.* **121,** 74 (1961).
22. B. G. Müller, *Z. Anorg. Allg. Chem.* **556,** 79 (1988).
23. D. Lorin, Doctorate Thesis, Université Bordeaux 1, France, 1980.
24. F. Schrötter and B. G. Müller, *Z. Kristallogr.* **196,** 261 (1991).
25. V. Wilhelm and R. Hoppe, *Z. Anorg. Allg. Chem.* **414,** 130 (1975).
26. G. Le Caër, Doctorate Thesis, Université Nancy 1, France, 1974.
27. K. P. Belov and A. N. Gozyaga, *Fig. Met. Metall.* **2,** 3 (1956).
28. J. S. Kouvel, Gen. El. Res. Lab. Report 57RL-1799 (1957).
29. A. Tressaud, F. Pintchovski, L. Lozano, A. Wold, and P. Hagenmuller, *Mater. Res. Bull.* **11,** 689 (1976).
30. E. O. Wollan, H. R. Child, W. C. Koehler, and M. K. Wilkinson, *Phys. Rev.* **112,** 1132 (1958).
31. A. J. Freeman, *in* "Proc. Conf. Neutron Scattering, Gatlinburg," Vol. 2, p. 592, 1976.
32. G. Lucier, S. H. Elder, L. Chacón, and N. Bartlett, *Eur. J. Solid State Inorg. Chem.* **33,** 809 (1996).
33. P. Day, C. Vettier, and G. Parisot, *Inorg. Chem.* **17,** 2319 (1978).
34. A. Tressaud, S. Khaïroun, J. M. Dance, and P. Hagenmuller, *Z. Anorg. Allg. Chem.* **517,** 43 (1984).